Reconstruction of spatial, phase, and coherence properties of light

Miroslav Ježek and Zdeněk Hradil

Department of Optics, Palacký University, 17. listopadu 50, 77200 Olomouc, Czech Republic

Received October 9, 2003; revised manuscript received February 5, 2004; accepted March 8, 2004

Image reconstruction of partially coherent light is interpreted as quantum-state reconstruction. An efficient method based on the maximum-likelihood estimation is proposed for acquiring information from blurred intensity measurements affected by noise. Connections with incoherent-image restoration are pointed out. The feasibility of the method is demonstrated numerically. Spatial and correlation details significantly below the diffraction limit are revealed in the reconstructed pattern. © 2004 Optical Society of America

OCIS codes: 030.1640, 100.3010, 100.5070, 100.6640, 100.6950, 110.4980.

1. INTRODUCTION

Light conveys a considerable amount of information about the environment. Information coded into and transmitted by light plays a crucial role in contemporary information technology. That is why any deeper understanding of fundamental limitations imposed by the theory represents a challenging problem. In particular, the resolution of the optical apparatus and the observation of phase objects are subjects of long-standing interest in the image-processing community. Both of these problems are related to the wave nature of light manifested by its ability to interfere. The scalar-wave theory represents an appropriate treatment of interfering optical signals.[1] We will restrict ourselves to the important case of quasi-monochromatic light. The ability to interfere as well as the spatial and phase properties of such a signal can be described by the correlation function of the second order, also called the mutual intensity.[1,2] Being the complex function of real two-point spatial coordinates, its modulus completely determines the intensity distribution and the degree of coherence of the light wave in space. Similarly, its argument determines the relative optical phase. Mutual intensity is all that we need for a complete description of the partially coherent scalar wave and its evolution and thus for a determination of the state of light in the framework of scalar-wave optics.

It is a well-known fact that the smallest distance of an object's details that can be resolved by an optical apparatus has a physical and not just a technical limit. The distance, called the diffraction limit, is proportional to the wavelength and inversely proportional to the angular distribution of the light observed in the output plane.[3] Hypothetically, we can restore such a corrupted image if we apply the inverse action of the optical apparatus. This direct approach to image restoration represents an intricate problem, the solution of which might be divergent and might even produce nonphysical results. Various regularizations and smoothing techniques have been devised to fix the problem.[4] However, some properties of the optical apparatus remain unknown in real observation. For example, imperfections in the optics and turbulence in the atmosphere both yield uncontrollable image degradation. All this is vaguely called noise. In addition to image restoration, resolution can be enhanced by eliminating out-of-focus light by means of the apodization technique[5] or by utilizing the confocal arrangement and interaction between light and matter, as in multiphoton fluorescence microscopy and the simulated emission depletion technique.[6,7]

Another fundamental physical restriction consists in the inability to observe a phase object without an interferometric setup. Direct observations are not able to determine the phase of the optical wave owing to its fast oscillations and the time integration of the intensity detectors. The phase must therefore be retrieved by adopting sophisticated techniques. This well-known phase problem[2] can be comprehended as a particular case of signal reconstruction. Let us define the reconstruction problem as a procedure for retrieving one physical quantity from the measurement of another one. We will review the basic methods of phase reconstruction in Section 4.

Let us assume the more realistic case of the reconstruction of a physical quantity in a plane different from the plane of the measurement. The reconstruction of the object intensity, optical phase, and coherence properties in the object (input) plane of the known optical apparatus from the corrupted intensity measured in the image (output) plane can serve as an example that occurs commonly in microscopy and astronomy. This task, which we consider in this paper, obviously unifies the problems of restoration and reconstruction. It seems to be infeasible to predict complex physical quantities such as phase and spatial correlations from the corrupted intensity data only. However, many different intensity measurements for various settings of the optical apparatus can be acquired and exploited for reconstruction of the complete state of the object. In the special case of phase-space tomography, the intensity measurements between the focus (Fourier) plane and the image plane of an ideal lens with infinite aperture determine the mutual intensity of the

1084-7529/2004/081407-10$15.00

input optical wave.[8] The method is sensitive to noise and can yield nonphysical results owing to the direct inversion of data.

In this paper the unified problem of restoration and reconstruction of the optical signal will be addressed from the viewpoint of statistical reconstruction techniques. The intensity measurements for several settings of a general optical apparatus will be used for the reconstruction of the mutual intensity of the partially coherent light. For the particular case of totally incoherent light, the proposed approach will be identified with the statistical Richardson algorithm[9] of image restoration.

There is a close analogy between scalar-wave optics and quantum theory. In the important case of a one pointlike particle propagating in space, the analogy is obvious.[8] Quantum theory describes the particle motion by means of a complex amplitude (de Broglie wave) involving interference effects. The intensity of the complex amplitude determines the probability of finding a particle. The same situation occurs in the scalar-wave optics. The coherent-light signal is described by a complex amplitude, the intensity of which is accessible by direct measurement. If we interpret this optical intensity as the probability of finding a photon, we reach the physical equivalence between quantum mechanics (de Broglie theory) and scalar-wave optics. Moreover, the well-known Planck relations,[10] $E = \hbar\omega$, $p = \hbar k$, link the energy and momentum of the photon with the angular frequency and wave number, respectively, of the corresponding optical scalar wave. The equivalence can be extended even to the case of a partially coherent signal described by the mutual intensity in scalar-wave optics and by the density operator in quantum mechanics.[8] This quantum-like approach will be briefly reviewed in Section 2. The problem of quantum-state reconstruction will be considered in analogy with the optical counterpart of image reconstruction in Section 5.

For the sake of simplicity, all the problems considered will be treated as two-dimensional problems. The first dimension corresponds to the longitudinal z coordinate, and the second dimension corresponds to the transverse x coordinate. Further generalization to higher dimensions can be obtained in a straightforward manner.

2. WAVE THEORY

In this section the analogy between scalar-wave optics and quantum mechanics will be highlighted. As will be shown, the abstract quantum formulation is advantageous for the purpose of signal reconstruction.

In the quantum domain, the pure quantum state $|\psi\rangle$ from Hilbert space[11] represents complete knowledge about the position and momentum of a particle, of course obeying the Heisenberg uncertainty principle.[10] Any randomness in the ensemble of identically prepared particles is described by the incoherent mixture of pure states—a density operator,

$$\hat{\rho} = \sum_k \lambda_k |\varphi_k\rangle\langle\varphi_k|. \tag{1}$$

Probabilities λ_k are nonnegative and add to unity, and the mixed state [Eq. (1)] satisfies the following relations,

$$\hat{\rho}^+ = \hat{\rho}, \qquad \mathrm{Tr}[\hat{\rho}] = 1, \qquad \langle\psi|\hat{\rho}|\psi\rangle \geqslant 0, \ \forall|\psi\rangle, \tag{2}$$

where $^+$ means the Hermitian conjugation. Denoting formally the position by a projector $|x\rangle\langle x|$, the complex amplitude $\psi(x) = \langle x|\psi\rangle$ describes the coherent quasi-monochromatic scalar field. Indeed, it characterizes the amplitude as well as the phase of the propagating wave. In the general case of a partially coherent field, the second-order correlation function,[2]

$$\Gamma(x, x') = \mathrm{Tr}[\hat{\rho}|x'\rangle\langle x|] = \sum_k \lambda_k \langle x|\varphi_k\rangle\langle\varphi_k|x'\rangle$$

$$= \sum_k \lambda_k \varphi_k(x)\varphi_k^*(x') = \langle\psi^*(x')\psi(x)\rangle_{\mathrm{ens}}, \tag{3}$$

describes the statistical properties of the field. The brackets $\langle\,\rangle_{\mathrm{ens}}$ denote the averaging over complex amplitudes of all modes k. The analogy between density operator (1) and mutual intensity (3) is expressed clearly by relations analogous to Eq. (2):

$$\Gamma^*(x', x) = \Gamma(x, x'), \qquad \int dx I(x) = 1,$$

$$\Gamma(x, x) \geqslant 0. \tag{4}$$

Note that the function $I(x) = \Gamma(x, x)$ means the optical intensity of the field. The analogy between quantum and wave descriptions can be emphasized in phase space by means of the Wigner quasi-distribution,[12,13]

$$W(x, p) = \frac{1}{\pi}\int dx' \exp(-i2px')\Gamma(x + x', x - x'). \tag{5}$$

This (x, p) distribution is a real bounded function, which is, however, not positively defined in general.

Let us proceed further to consider the state transformation. Assuming linearity and causality, the equation for evolution of a pure state formally reads

$$|\psi\rangle_{\mathrm{out}} = \hat{T}|\psi\rangle_{\mathrm{in}}. \tag{6}$$

Here $\hat{T}$ is linear operator satisfying the equation

$$\frac{\partial}{\partial z}\hat{T} = \hat{L}\hat{T}, \tag{7}$$

where z is evolution parameter and the generator $\hat{L}$ of the evolution is considered to be z independent. Evolution equation (7) covers both the Schrödinger equation in quantum mechanics and the paraxial Helmholtz equation in the Fresnel approximation of scalar-wave optics. The unitary evolution is governed by the Hamiltonian operator $\hat{L} = -(i/\hbar)\hat{H}$, and the evolution of the mixed state is described by the transformation

$$\hat{\rho}_{\mathrm{out}} = \hat{T}\hat{\rho}_{\mathrm{in}}\hat{T}^+, \qquad \hat{T} = \exp\left(-\frac{i}{\hbar}\hat{H}z\right). \tag{8}$$

Evolution (8) of the state $\hat{\rho}$ in the Schrödinger picture can be equivalently formulated in the Heisenberg picture. This formulation follows the laws of ray optics. Indeed, the relationship between the canonical observables of position and momentum reads

$$\begin{pmatrix} \hat{x}_{\mathrm{out}} \\ \hat{p}_{\mathrm{out}} \end{pmatrix} = \hat{T}^{+} \begin{pmatrix} \hat{x}_{\mathrm{in}} \\ \hat{p}_{\mathrm{in}} \end{pmatrix} \hat{T}. \tag{9}$$

In particular, for the evolution generated by the quadratic Hamiltonian in canonical observables, transformation (9) is linear,

$$\begin{pmatrix} \hat{x}_{\mathrm{out}} \\ \hat{p}_{\mathrm{out}} \end{pmatrix} = T \begin{pmatrix} \hat{x}_{\mathrm{in}} \\ \hat{p}_{\mathrm{in}} \end{pmatrix} = \begin{bmatrix} A & B \\ C & D \end{bmatrix} \begin{pmatrix} \hat{x}_{\mathrm{in}} + s \\ \hat{p}_{\mathrm{in}} + r \end{pmatrix}, \tag{10}$$

where $\mathrm{Det}[T] = AD - BC = 1$. This generic $ABCD$ transformation covers useful cases of wave transformation, for example free evolution, displacement, rotation, phase shift, squeezing, and chirp. Linear transformation of the $(\hat{x}, \hat{p})$ operators induces the evolution of the Wigner function by linear transformation of its variables,

$$W(x, p) = W(Dx - Bp - s, -Cx + Ap - r). \tag{11}$$

Roughly speaking, all these transformations rotate and rescale the input state. As a consequence, the observable $A\hat{x} + B\hat{p}$ can be measured, offering an important tool for all the tomographic methods.

In the classical limit there is a close connection between the evolution of the position and momentum operators in the Heisenberg picture [Eq. (10)] and geometrical paraxial optics represented by the identity between operators $(\hat{x}, \hat{p})$ and their c values (x, p). The state vector (x, p) is used to specify the position and angle of the optical ray. A similar description may be adopted for particles in classical mechanics. The evolution operator $\hat{T}$ is given by the $ABCD$ matrix T completed by the transverse shift s and rotation r in analogy with relation (10). Geometrical optics as well as classical mechanics do not involve interference, which simplifies the input–output relations considerably. This is why geometrical optics is so suitable for "direct" observations. Indeed, if the positions x_1, x_2 for two values z_1, z_2 are measured, the state vector (x_0, p_0) for $z = 0$ can be completely reconstructed as

$$\begin{pmatrix} x_0 \\ p_0 \end{pmatrix} = \frac{1}{z_2 - z_1} \begin{pmatrix} x_1 z_2 - x_2 z_1 \\ x_2 - x_1 \end{pmatrix}. \tag{12}$$

In the case of losses, the evolution turns out to be nonunitary. Let us imagine the absorbing screen with aperture $2a$. The incident state can be decomposed in the base of eigenstates $|\xi\rangle$ of position $\hat{x}$ on the screen. Since only a part of the eigenstate spectrum for eigenvalues $\xi \in [-a, a]$ is transmitted, the nonunitary transformation can be described by the projection operator

$$\hat{T} = \int_{-a}^{a} \mathrm{d}\xi |\xi\rangle\langle\xi| \tag{13}$$

corresponding to the finite aperture.

Let us conclude the overview by an explicit formulation of the state transformation in position representation. The generic evolution [Eq. (6)] of the pure state (coherent wave) takes the well-known form of the superposition integral,

$$\psi_{\mathrm{out}}(x) = \langle x|\,\psi\rangle_{\mathrm{out}} = \int \mathrm{d}x_0 \langle x|\hat{T}|x_0\rangle\langle x_0|\,\psi\rangle_{\mathrm{in}} = \int \mathrm{d}x_0 h(x, x_0)\psi_{\mathrm{in}}(x_0). \tag{14}$$

The kernel of integral transformation (14),

$$h(x, x_0) = \langle x|\hat{T}|x_0\rangle, \tag{15}$$

is called the propagator in quantum theory and the response function or point-spread function in scalar-wave theory.[3] Loosely speaking, it relates the point source in the object (input) plane $z = 0$ with its image in the image (output) plane. This mapping is fuzzy in realistic image processing owing to the effect of diffraction caused by nonunitary evolution. In the case of an unlimited aperture it may become sharp, corresponding to the case of unitary evolution, $\hat{T}^{+} = \hat{T}^{-1}$. Analogously, evolution (8) of the mixed state (mutual intensity) in the position representation reads[2]

$$\Gamma_{\mathrm{out}}(x, x') = \int\int \mathrm{d}q\,\mathrm{d}q' h(x, q) h^{*}(x', q')\Gamma_{\mathrm{in}}(q, q'). \tag{16}$$

3. DETECTION

According to the standard formulation of quantum mechanics, a measurement is represented by an observable,[10] a Hermitian operator $\hat{A}$. Eigenvalues of this operator correspond to possible results of elementary measurements. Eigenstates determine the possible states after the measurement, and they are complete and orthogonal:

$$\hat{A}|a\rangle = a|a\rangle, \qquad \sum_{a} |a\rangle\langle a| = \hat{1}, \qquad \langle a|a'\rangle = \delta_{aa'}. \tag{17}$$

These properties are reflected in the probability $p_a = \mathrm{Tr}[\hat{\rho}|a\rangle\langle a|]$ predicted by quantum theory guaranteeing the normalization of probabilities $\Sigma_a p_a = 1$ (completeness) and mutual exclusivity of the results a (orthogonality). This description may be further generalized in terms of a positive-operator-valued measure (POVM) yielding the decomposition of the identity operator,[14,15]

$$\hat{\Pi}_b \geqslant 0, \qquad \sum_{b} \hat{\Pi}_b = \hat{1}, \tag{18}$$

which predicts the probability for registering the output b analogously to the case of orthogonal projectors, $p_b = \mathrm{Tr}[\hat{\rho}\hat{\Pi}_b]$. The notion of POVM plays a crucial role in the description of a generic quantum measurement in state estimation and discrimination.

Registration of the image intensity $I(x)$ of a partially coherent wave in the transverse position x corresponds to the measurement of the position operator $\hat{x}$ in the output plane:

$$I(x) = \Gamma_{\mathrm{out}}(x, x) = p(x) = \mathrm{Tr}[\hat{\rho}_{\mathrm{out}}|x\rangle\langle x|]. \tag{19}$$

The realistic detector always possesses finite spatial resolving power. With its pixels denoted by the indices i, the simplest representation of detector's POVM is given by the operators

$$\hat{O}_i = \int_{\Delta_i} \mathrm{d}x |x\rangle\langle x|, \tag{20}$$

where the integration is done along the surface of the ith pixel.

Consider now the generic observation scheme. The input state $\hat{\rho}$ represented by its mutual intensity $\Gamma(x, x')$ in the wave-theory framework is transformed by the optical device $\hat{T} = \hat{T}(A, B, \ldots)$ with the response function $h(x, x_0; A, B, \ldots)$. The resulting output state $\hat{\rho}_{\mathrm{out}}$ is observed by the intensity detector [Eq. (20)] placed in the output plane. The detector counts the elementary clicks in every ith pixel. The number N_i of registered clicks determines the relative frequency $f_i = N_i/N$, $N = \Sigma_i N_i$ of the pixel response. These measured data f_i sample the probabilities p_i (intensities I_i):

$$p_i = \mathrm{Tr}[\hat{\rho}_{\mathrm{out}}\hat{O}_i] = \mathrm{Tr}[\hat{\rho}\hat{\Pi}_i], \qquad \hat{\Pi}_i = \hat{T}^{+}\hat{O}_i\hat{T}. \tag{21}$$

Note, however, that this scheme is rather classical and does not take into account statistics of the detection process in accordance with classical optics, in which intensity is considered a measurable quantity. Provided that the quantum nature of detection is considered, relation (20) should be modified by taking into account the registration of photons instead.

4. DIRECT INVERSION

The restoration and reconstruction of the signal in wave theory is a rather complex and extensive field with many applications. Let us briefly review this topic. Assuming an unknown signal propagating through optical refractive and diffractive elements, the output field may be detected. Provided that the properties of the optical device are known and detection is ideal, the input signal may be predicted from the output one. This is the classical problem of image restoration.

Standard methods use the isoplanatic approximation involving relation (14) as convolution:

$$\psi_{\mathrm{out}} = \int \mathrm{d}x_0 h(x - x_0)\psi_{\mathrm{in}}(x_0)\,. \tag{22}$$

Inversion is given by the Fourier deconvolution:

$$\tilde{\psi}_{\mathrm{in}} = \frac{\tilde{\psi}_{\mathrm{out}} + \tilde{\mathcal{N}}}{\tilde{h}}. \tag{23}$$

Here $\tilde{\psi}_{\mathrm{in}}$, $\tilde{\psi}_{\mathrm{out}}$, and $\tilde{h}$ are Fourier transformations of ψ_{in}, ψ_{out}, and h, respectively, and $\tilde{\mathcal{N}}$ represents the spectrum of the additive noise $\mathcal{N}$. The typical point-spread function h has the form of a sinc or a besinc function, and $\tilde{h}$ corresponds to a step function. Hence the spatial frequencies of the signal are transmitted only up to a certain upper cutoff.[3] This is why the deconvolution is very sensitive to the noise $\mathcal{N}$ and diverges at spatial frequencies for which the transfer function $\tilde{h}$ turns out to be zero. In particular, for frequencies above the cutoff, the transfer function $\tilde{h}$ vanishes and Eq. (23) diverges owing to the broad noise spectrum $\tilde{\mathcal{N}}$. Some regularization procedures are necessary in all these cases.[4,16–22] Special attention has been devoted to a more accurate description of the optical device. A detailed analysis requires a special choice of eigenfunctions related to the finite aperture instead of spatial frequencies.[23–25] A systematic theory of this remarkable basis, called prolate spheroidal wave functions, was given by Frieden.[26] Several further superresolution techniques such as apodization[5] and analytic continuation[27,28] have been suggested.

Another problem arises if we take into account a further realistic aspect of detection, namely, the inability of the intensity detector to observe the phase and coherence properties of the optical signal. Missing information is the subject of reconstruction, as we briefly discussed in Section 1. A large number of phase-retrieval algorithms have been devised because of the long-standing interest in the observation of phase objects. Earlier approaches rely on mathematical properties of the optical signal and use analytic continuation.[2,27,29,30] These methods enable us to reconstruct the optical phase as well as the coherence properties. Unfortunately, they are very sensitive to noise and often produce nonphysical results. The well-known Gerchberg–Saxton method[31] and other methods of projection onto convex sets[32–36] use the intensity measurement in the focus (Fourier) plane. The Gerchberg–Saxton algorithm is relatively robust but does not converge in all cases.[32,36] Another feasible method of phase reconstruction relies on solving the transport-of-intensity equation.[37–41] It is the linear nonseparable partial differential equation of the second kind, the solving of which is very inconvenient. Moreover, the phase must satisfy the boundary conditions, which are not known *a priori*. Further methods use the direct inversion of various analytical relations between intensity and phase distributions. The phase reconstruction from the intensity measurements in two planes connected by a small canonical transformation can serve as an example.[42]

Standard image restoration and reconstruction deal mainly with the observation in the image plane that reveals the sharpest image. However, the observations in defocused planes are also worthwhile.[8,41,43,44] They correspond to the observation of $A\hat{x} + B\hat{p}$ operators in the language of quantum theory [Eq. (10)], providing another piece of information about the signal and affording better employment of measured data. Such a tomographic technique was suggested by Bertrand and Bertrand[45] and Vogel and Risken[46] in the quantum domain and was verified experimentally by a group from the University of Oregon.[47] The same group proposed the tomographic reconstruction of the mutual intensity based only on refractive optics.[8] The method relies on intensity measurements between the image plane and the focus (Fourier) plane of an ideal lens with infinite aperture. The simplified version of this method was confirmed by an experiment with de Broglie waves of helium atoms.[48] Several other tomographic schemes for observing various facets of the system have been proposed. These have usually been achieved by adjusting some of the parameters in the setup. Particular configurations depending on the pa-

rameter provide the desired group of transformations. Classical x-ray tomography used in medicine,[49–51] various knife-edge methods,[52] and quantum tomography[46,47,53–57] use the group of rotations. Phase-space tomography and chronocyclic tomography are related to the symplectic group, but they are convertible to classical tomography.[8,43] General nonhomogeneous symplectic tomography was introduced by Mancini *et al.*[58] and Man'ko.[59]

All the above-mentioned direct methods of restoration and reconstruction relate measured data f_i to theoretical probabilities p_i by means of the equality

$$\mathrm{Tr}[\hat{\rho}\hat{\Pi}_i] = f_i, \tag{24}$$

where the multi-index i passes over all configurations of the optical apparatus and over all pixels of the detector. However, the solution of linear equations (24) represents an ill-posed problem. The solution is very sensitive to noise, which is inevitably involved in any measurement scheme. "Ill-posed problem" implies that the reconstructed "state" need not represent any physically possible object. In the language of quantum theory this means that $\langle \psi|\hat{\rho}|\psi\rangle < 0$ may hold for some states $|\psi\rangle$. Alternatively, the reconstructed optical intensity $I(x)$ may drop below zero for some spatial coordinates in the wave-theory framework. Linear algorithms are not able to guarantee such necessary conditions as positive definiteness of the density operator or mutual intensity.

Statistical approaches suggest a remedy to this problem, removing the strict condition of Eq. (24). For example, the equality between f_i and p_i could be replaced by the requirement of their minimal least-squares difference,

$$\sum_i |f_i - \mathrm{Tr}[\hat{\rho}\hat{\Pi}_i]|^2, \tag{25}$$

an obvious choice in engineering practice. The least-squares method has been applied to the restoration of optical intensity[60,61] as well as to the complete reconstruction of the quantum state represented by a density operator.[62] Nevertheless, other metrics are also possible. Richardson's method[9] based on the Bayesian approach proves to be a powerful technique for incoherent image reconstruction. The maximum-likelihood principle and the expectation-maximization algorithm[63] originated in Fisher's work.[64,65] They are of fundamental importance in numerous areas of signal processing, such as emission tomography,[66–68] absorption tomography,[69,70] and incoherent-image restoration.[71] The minimum Fisher information and the prior principle of the maximum Cramer–Rao bound both can be applied to optics and quantum theory.[72–74] The maximum-entropy principle[75,76] represents another useful statistical tool for intensity restoration[77–79] and quantum-state estimation.[80] The feasibility of all the mentioned methods has been confirmed. However, the optical phase and coherence properties of the scalar-wave signal are not retrieved by any of these methods. Indeed, these methods restore only the corrupted optical intensity or, alternatively, compose the incoherent image from tomographic data. In the following section a unified restoration and reconstruction method based on maximum likelihood will be proposed to reconstruct the mutual intensity from several intensities corrupted by the general optical apparatus and by additional noise.

5. RECONSTRUCTION AS GENERALIZED QUANTUM MEASUREMENT

Let us assume the generic scheme of quantum measurement [Eqs. (20) and (21)] described in Section 3. The conditional probability of detecting N_i clicks in the ith pixel if the state $\hat{\rho}$ occurs in the input plane has the form of multinomial distribution,

$$\mathcal{L}(\hat{\rho}) \approx \prod_i p_i^{Nf_i}, \tag{26}$$

where the measured data are represented by relative frequencies f_i of the registered clicks, $Nf_i = N_i$, and p_i mean the probabilities (intensities) predicted by theory (21). The multi-index i denotes the configuration of the optical apparatus and the pixel of the detector. The input state $\hat{\rho}$ is the subject of the estimation procedure. The likelihood functional [Eq. (26)] then answers the question "How is it likely that the given data f_i were registered provided that the system was in the given quantum state $\hat{\rho}$?" The detection of given data is more likely for some states than for others. Using relation (21), we obtain the log-likelihood functional:

$$\ln \mathcal{L}(\hat{\rho}) = \sum_i f_i \ln p_i = \sum_i f_i \ln \mathrm{Tr}[\hat{\rho}\hat{\Pi}_i]. \tag{27}$$

The maximum-likelihood principle selects such a state $\hat{\rho}_{\mathrm{est}}$ for which the likelihood reaches its maximum:

$$\hat{\rho}_{\mathrm{est}} = \arg\max_{\hat{\rho}} \ln \mathcal{L}(\hat{\rho}). \tag{28}$$

Being the convex functional of the state $\hat{\rho}$, likelihood (27) possesses only one maximum or only one plateau of maxima. The formal necessary condition for this global maximum,

$$\left.\frac{\delta \ln \mathcal{L}(\hat{\rho})}{\delta \hat{\rho}}\right|_{\hat{\rho}_{\mathrm{est}}} = 0, \tag{29}$$

may be rewritten in the form of the extremal operator equation,[81–85] or, alternatively, extremization can be done by means of the numerical uphill simplex method.[86] Any density operator may be parameterized in the diagonal form [Eq. (1)] by using independent (orthogonal) basis states $|\varphi_k\rangle$, and the variation [Eq. (29)] may be done along these rays. The likelihood functional depends on the density operator through probabilities p_i. This yields the system of coupled equations $[\delta \ln \mathcal{L}(\hat{\rho})]/(\delta\langle\varphi_k|) = 0$ for any allowed component k. Using the relation

$$\frac{\delta \ln \mathcal{L}(\hat{\rho})}{\delta\langle\varphi_k|} = \sum_i \frac{f_i}{p_i}\hat{\Pi}_i|\varphi_k\rangle \tag{30}$$

and the normalization $\mathrm{Tr}[\hat{\rho}] = 1$, we obtain the extremal equation[81–85]:

$$\hat{R}\hat{\rho} = \hat{\rho}. \tag{31}$$

Here

$$\hat{R} = \sum_i \frac{f_i}{p_i}\hat{\Pi}_i, \tag{32}$$

and the probabilities p_i are state dependent [Eq. (21)]. Operator equation (31) determines the most likely solution $\hat{\rho}_{\mathrm{est}}$, for which $\hat{R}(\hat{\rho}_{\mathrm{est}}) = \hat{1}$ holds on the Hilbert space of the state $\hat{\rho}_{\mathrm{est}}$.[81,84] No prior knowledge about the estimated state is needed; results of the measurement itself are sufficient for analysis.

Let us develop the optical counterpart of this reconstruction problem. In the spatial domain extremal equation (31) has the form of the integral equation for the mutual intensity $\Gamma(x, x')$,

$$\int \mathrm{d}x' \mathcal{R}(q, x')\Gamma(x', q') = \Gamma(q, q'), \tag{33}$$

where the resolution of identity $\hat{1} = \int \mathrm{d}x|x\rangle\langle x|$ has been used. The kernel

$$\mathcal{R}(q, x') = \sum_i \frac{f_i}{p_i}\mathcal{P}_i(q, x') \tag{34}$$

and the functions

$$\mathcal{P}_i(q, x') = \int_{\Delta_i} \mathrm{d}x h^*(x, q)h(x, x') \tag{35}$$

correspond to the operator $\hat{R}$ and to the POVM operators $\hat{\Pi}_i$, respectively. Probabilities (21) of the elementary detections in the individual pixels then read

$$p_i = \int\int \mathrm{d}q\,\mathrm{d}q'\Gamma(q, q')\mathcal{P}_i(q', q). \tag{36}$$

Equation (33) relates the measured data f_i, properties of the optical apparatus, and the reconstructed signal $\Gamma(x, x')$. Dependence on the optical apparatus is expressed through the point-spread function $h(x, x')$ only. However, this mutual relation is inseparable, since the relation is nonlinear. In contrast to standard treatments in scalar-wave optics, no assumptions about the statistical nature of the signal have been made. This seems reasonable, since the coherence properties of the light field may change during propagation (the van Cittert–Zernike effect[2]). The proposed formulation anticipates only knowledge of the optical apparatus and the measured data without any prior assumptions about the unknown signal.

Special cases of the generic formulation deserve attention. Let us consider an iterative solution of Eq. (33) taking the maximally ignorant initial guess represented by the totally mixed state, $\hat{\rho}^{(0)} = (1/D)\hat{1}$, where $1/D$ ensures the trace normalization in D-dimensional Hilbert space. This corresponds to the totally incoherent optical signal with uniform intensity. After evaluating the kernel $\hat{R}^{(0)}$ we are able to write down the first iteration of the estimated state, $\hat{\rho}^{(1)} = \hat{R}^{(0)}\hat{\rho}^{(0)} = \Sigma_i f_i\hat{\Pi}_i/\mathrm{Tr}[\hat{\Pi}_i]$. In the spatial domain this state has the form of the partially coherent superposition of response functions [Eq. (15)] weighted by the measured data f_i, $\Sigma_i f_i = 1$:

$$\Gamma^{(1)}(q, q') = \sum_i f_i \frac{\int_{\Delta_i} \mathrm{d}x h^*(x, q)h(x, q')}{\int \mathrm{d}\xi \int_{\Delta_i} \mathrm{d}x|h(x, \xi)|^2}. \tag{37}$$

Obviously, the coherence properties of the estimated signal are changed during repeated iterations of extremal equation (33):

$$\Gamma^{(n+1)}(q, q') = \int \mathrm{d}x'\mathcal{R}^{(n)}(q, x')\Gamma^{(n)}(x', q'). \tag{38}$$

The convexity of the likelihood functional on the convex set of mutual intensities ensures convergence to the global maximum. In addition to the proposed iterative solution, the well-known expectation-maximization algorithm[63] completed by the unitary step[84] can also be utilized. This guarantees convergence and keeps all fundamental properties [Eq. (4)] of the partially coherent signal $\Gamma(x, x')$.

As the second special case, the totally incoherent light can be assumed,

$$\Gamma(x, x') = I(x)\delta(x - x'), \tag{39}$$

where $\delta(x)$ is the Dirac distribution. The extremal equation then reduces to

$$\int \mathrm{d}q'\mathcal{R}(q, q')I(q') = I(q), \tag{40}$$

and probabilities (36) read

$$p_i = \int \mathrm{d}q\mathcal{P}_i(q, q)I(q). \tag{41}$$

Relations (40), (34), and (41) provide the extremal equation for the unknown optical intensity $I(x)$:

$$\sum_i \frac{f_i}{\int \mathrm{d}q\mathcal{P}_i(q, q)I(q)} \int \mathrm{d}q'\mathcal{P}_i(x, q')I(q') = I(x). \tag{42}$$

This equation may be utilized for the iterative procedure as was proposed by Richardson in 1972 for incoherent-image restoration. It is worth noting that in the original derivation[9] the Bayes rule was adopted. The treatment devised here makes it possible to extend the Bayesian solution to the case of partially coherent signal reconstruction.

6. NUMERICAL EXAMPLE

In this section we use a carefully selected example to demonstrate the feasibility and advantages of the presented method. A partially coherent testing object is chosen below the resolution limit of a simple optical device with finite aperture. Therefore, the corrupted output intensities do not bear any resemblance to the true object. Furthermore, a great deal of background noise is added to these simulated data. In spite of these obvious limitations the reconstructed object reveals the original structure. This improvement is achieved by using the output intensities for several transverse and longitudinal positions of the object.

Let us consider an optical setup that consists of free evolution at a distance d_{in}, a thin lens with focal length f, and free evolution at a distance d_{out}. The lens has an aperture diameter $2a$. The whole device can be transversely shifted at a distance s from the axial position. The longitudinal distance d_{in} from the object and the transverse shift s are parameters of the optical setup and may be adjusted during measurement, and the other parameters are kept constant. The point-spread function $h(x, x_0) = h(x, x_0; d_{\text{in}}, s) = \langle x|\hat{T}(d_{\text{in}}, s)|x_0\rangle$ of the device under consideration reads

$$h(x, x_0) = \langle x|\exp\left(-\mathrm{i}\frac{d_{\text{out}}}{2k}\hat{p}^2\right)\int_{-a}^{a}\mathrm{d}\xi|\xi\rangle\langle\xi| \times \exp\left(-\mathrm{i}\frac{k}{2f}\hat{x}^2\right)\exp\left(-\mathrm{i}\frac{d_{\text{in}}}{2k}\hat{p}^2\right) \times \exp(-\mathrm{i}s\hat{p})|x_0\rangle, \tag{43}$$

where $k = 2\pi/\lambda$ is the longitudinal wave number. With the help of the relations $\hat{1} = \int \mathrm{d}x|x\rangle\langle x|$, $\hat{1} = \int \mathrm{d}p|p\rangle\langle p|$, and $\langle x|p\rangle = (2\pi)^{-1/2}\exp(\mathrm{i}xp)$, the point-spread function [Eq. (43)] can be rewritten in the form

$$h(x, x_0) = h_\infty(x, x_0)\mathcal{E}(x, x_0). \tag{44}$$

Here

$$h_\infty(x, x_0) = \exp\left\{\mathrm{i}\frac{k}{2}\left[\left(\frac{x^2}{d_{\text{out}}} + \frac{(x_0 + s)^2}{d_{\text{in}}}\right) - \frac{\theta^2}{\Delta}\right]\right\} \tag{45}$$

is the response function of the ideal refractive focusing device and

$$\mathcal{E}(x, x_0) = \frac{1}{2}\mathrm{erf}\left[\frac{1 - \mathrm{i}}{2}\sqrt{k\Delta}\left(\frac{\theta}{\Delta} + a\right)\right] - \frac{1}{2}\mathrm{erf}\left[\frac{1 - \mathrm{i}}{2}\sqrt{k\Delta}\left(\frac{\theta}{\Delta} - a\right)\right] \tag{46}$$

represents the correction to the finite aperture, which tends to unity for large aperture, $\lim_{a\to\infty}\mathcal{E}(x, x_0) = 1$. The parameter Δ characterizes the defocusing from the imaging configuration,

$$\Delta = 1/d_{\text{in}} + 1/d_{\text{out}} - 1/f, \tag{47}$$

the parameter θ is related to the transverse wave number,

$$\theta = \theta_{\text{in}} + \theta_{\text{out}} = \frac{x_0 + s}{d_{\text{in}}} + \frac{x}{d_{\text{out}}}, \tag{48}$$

and the function erf( ) denotes the common error function,

$$\mathrm{erf}(z) = \frac{2}{\sqrt{\pi}}\int_0^z \mathrm{d}t\,\exp(-t^2). \tag{49}$$

In the present simulation the parameters have been chosen as $\lambda = 600\,\text{nm}$, $d_{\text{out}} = 1.5\,\text{m}$, $f = 0.5\,\text{m}$, and $a = 0.6\,\text{mm}$. The image ($\Delta = 0$) appears in the output plane in the case $d_{\text{in}} = 0.75\,\text{m}$. However, it is blurred owing to the small aperture. Strictly speaking, details closer than the diffraction limit

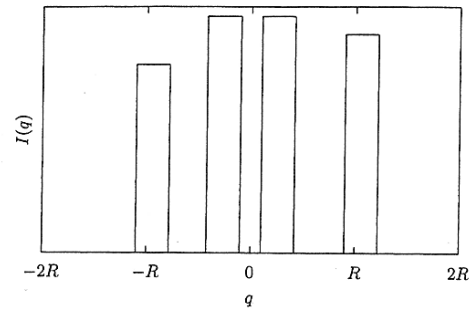

Fig. 1. Optical intensity $I(q)$ of the true object in the input plane.

$$R = C\lambda d_{\text{out}}/a \tag{50}$$

are mapped to two spots with an insufficient contrast according to Rayleigh's criterion. The factor C depends on the aperture shape and the coherence properties of the signal. It equals 0.61 in the case of circular shape and totally incoherent light or 0.82 in the case of totally coherent light (Abbé's resolution limit). We set $C = 0.5$, which is equal to or smaller than any classical resolution limit for imaging with partially coherent light. The testing object in the input plane consists of four bright spots separated by dark spaces. The distance 0.15 mm between the edges of the central closest spots is five times smaller than the resolution limit [Eq. (50)], $R = 0.75\,\text{mm}$. The width of the spots is 0.25 mm. The corresponding optical intensity $I(q)$ in the input plane is shown in Fig. 1. The off-diagonal peaks of the mutual intensity $\Gamma(q, q')$ of the testing object, representing the cross correlations between the spots, are lower than diagonal ones, owing to the partial coherence. The contrast $\mathcal{V} = (I_{\max} - I_{\min})/(I_{\max} + I_{\min})$ of the object is $\mathcal{V} = 1$.

The object plane q is discretized by 100 equidistant points in the interval $[-1.5, 1.5]$ mm or, equivalently, $[-2R, 2R]$. The corresponding mutual intensity $\Gamma(q, q')$ is given on a square mesh of 100×100 points (q_m, q_n') in the process of data generation and subsequent reconstruction. It is determined by $100^2 - 1$ independent unknown real numbers, according to properties (4). Similarly, the detection (output) plane x in the interval $[-4, 4]$ mm is sampled by 64 pixels x_i for every longitudinal distance $d_{\text{in}j} = (0.75 - 0.05j)\,\text{m}$, $j = 0,\ldots,5$, and for every transverse shift $s_l = (-1.2 + 0.3l)\,\text{mm}$, $l = 0,\ldots,8$. With relations (35), (36), and (44)–(46), the intensities $p_{ijl} = I_{jl}(x_i)$ in the pixels i can be evaluated for all the configurations (j, l) of the optical setup. For example, in the case of the imaging axial configuration ($j = 0, l = 4$), the intensity reveals the central peak with small sidelobes; see Fig. 2. The corresponding undersampled data f_i spoiled by 20% background noise are shown in the same figure. The total number of approximately 3500 simulated data f_{ijl} serves as an input for the reconstruction procedure [Eqs. (33)–(35)]. Thus the number of data does not reach the number of the unknown estimated parameters, but they are of the same order. To solve extremal equation (33) we need to find the mutual intensity on the given mesh as a Hermitian matrix of the dimension 100×100, by means of repeated iterations (38). As an initial iteration $\Gamma^{(0)}$, the uniform in-

coherent superposition of all pure states on the considered space is used; it exhibits a flat intensity profile. It is important to note that the final result seems to be independent of the choice of the initial mutual intensity. With the help of $\Gamma^{(0)}$ and Eqs. (36), (35), and (34), we obtain the kernel $\mathcal{R}^{(0)}$. Subsequently, relation (38) for $n = 0$ yields the first iteration $\Gamma^{(1)}$ of mutual intensity (37), and so on. In the course of the repeated iterations of the discretized equation (38) the difference $\epsilon = \Sigma_{mn}|\Gamma^{(n+1)}(q_m, q_n') - \Gamma^{(n)}(q_m, q_n')|^2$ between two successive iterations can be used as the criterion for terminating the extremization process. Numerical results show that the square difference ϵ reaches a level of $\sim 10^{-6}$ after several tens of iterations and reaches a level of $\sim 10^{-12}$ after approximately 1000 iterations; see Fig. 3. The limit $\epsilon \to 0$ is equivalent to the convergence of $\Gamma^{(n)}$ to the optimal solution owing to the convexity of likelihood functional (27). The iterated intensity starts to reveal the four-peak structure after a relatively small number of steps. The contrast $\mathcal{V}$ of the central part of the estimated optical intensity beyond the diffraction limit R reaches a value of 0.56 after 1000 iterations; see Fig. 4. The positions and relative intensities of the bright spots and their correlations in the estimated object match the structure of the true object very well, as demonstrated in Fig. 5. The relative optical phase between the closest central peaks of the mutual intensity is $\phi = \arg\Gamma(-0.2\,\text{mm}, 0.2\,\text{mm}) = 0$ rad for the original object and -0.022 rad for the reconstructed one. This corresponds to a relative-phase error <0.5%.

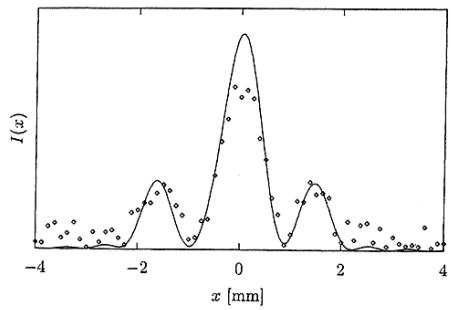

Fig. 2. Simulated data f_i in 64 pixels (points) affected by 20% background noise sample the optical intensity $I(x)$ in the output plane (curve) for imaging axial arrangement, $d_{\text{in}} = 0.75$ m, $s = 0$.

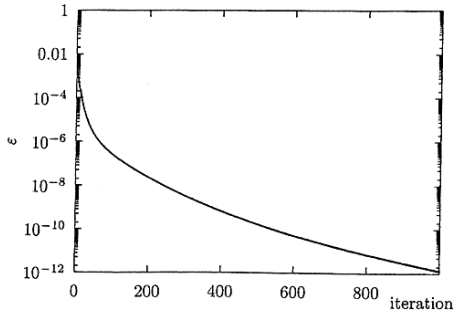

Fig. 3. Exponentially fast convergence of the square difference ϵ between two successive iterations during the extremization process.

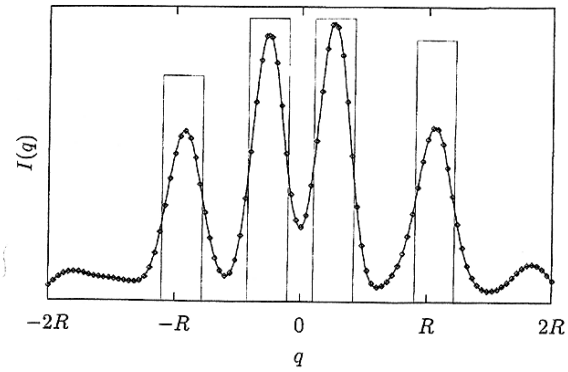

Fig. 4. Optical intensity $I(q)$ of the reconstructed object in the input plane (points) compared with the true object (thin lines).

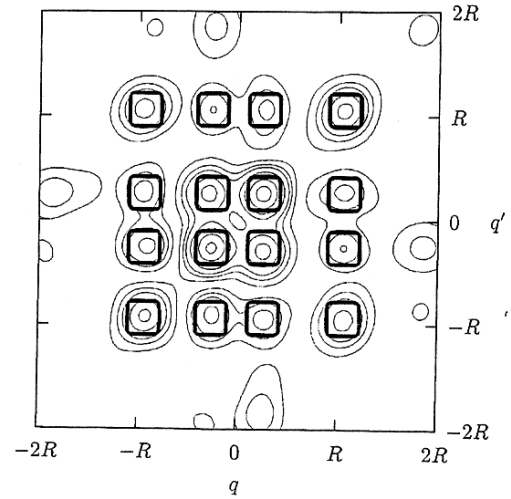

Fig. 5. Contour lines (thin lines) of the reconstructed mutual intensity $\Gamma(q, q')$. The positions of the diagonal-intensity spots as well as the positions of the off-diagonal correlations match the true ones (thick lines).

The numerical simulations clearly show that the proposed reconstruction algorithm is feasible and can be implemented. It provides considerable improvement over nonstatistical image-processing techniques, and, significantly, it yields complete information in the form of the correlation function. Similarly, in the quantum domain the particular realizations of the presented algorithm have been applied successfully to the reconstruction of the spin state[84,87] and to homodyne tomography.[88,89]

7. CONCLUSION

The purpose of this paper is twofold. First the close connection between wave optics and quantum mechanics has been emphasized. The operator language routinely used in quantum theory can simplify the manipulation and description of optical objects, such as partially coherent waves and response functions of optical devices. The second goal is the mathematical formulation of the reconstruction algorithm for partially coherent signals proceeding from the maximum-likelihood estimation of mixed quantum states.[81–85] The solution of the extremal equation by means of repeated iterations has been suggested.

The first iteration has been explicitly formulated. The proposed method never yields nonphysical results.

The feasibility of the method has been verified by extensive numerical simulations. Realistic experimental data will be considered in a forthcoming publication. The particular numerical example shows good agreement between the true and the estimated states of partially coherent light beyond the diffraction limit, despite undersampled data and 20% background noise.

The method is able to estimate a generic signal without any prior assumptions, utilizing real noisy data only. The potential applications cover a wide range of restoration and reconstruction problems. The method can be used for the state estimation of the localized mode in photonic bandgap structures (photonic crystals), for the determination of correlations of the signal transmitted through random media and for the reconstruction of spatial and coherence properties of light confined and emitted by modern laser-diode sources. Moreover, the general quantum origin of the method allows us to estimate an arbitrary, continuous (discretized), partially coherent physical object described by the correlation function or the Wigner function. The reconstruction of the de Broglie wave of a particle and the optical homodyne detection of a quantum state of the light mode are typical examples. In short, the method is applicable to all inverse problems in which precise knowledge of the partially coherent signal (mixed state) is essential, provided that the measurement device and real data are known.

ACKNOWLEDGMENTS

We thank Z. Bouchal, J. Fiurášek, and J. Wagner for valuable discussions. This work was supported by the Czech Ministry of Education under the projects OC P11.003, "Physics of linear, nonlinear and active photonic crystals," in the framework of European Union grant COST-P11 and LN00A015, "Research Centre for Optics."

Miroslav Ježek's e-mail address is jezek@optics.upol.cz.

REFERENCES

1. M. Born and E. Wolf, *Principles of Optics*, 6th ed. (Pergamon, New York, 1980), Chap. X.
2. J. Peřina, *Coherence of Light*, 2nd ed. (Reidel, Dordrecht, The Netherlands, 1985).
3. J. W. Goodman, *Introduction to Fourier Optics*, 2nd ed. (McGraw-Hill, New York, 1996).
4. M. Bertero and P. Boccacci, *Introduction to Inverse Problems in Imaging* (IOP, London, 1998).
5. P. Jacquinot and B. Roizen-Dossier, "Apodisation," in *Progress in Optics, Vol. III*, E. Wolf, ed. (North-Holland, Amsterdam, 1964), Chap. 2, pp. 29–186.
6. M. Dyba and S. W. Hell, "Focal spots of size λ/23 open up far-field fluorescence microscopy at 33 nm axial resolution," Phys. Rev. Lett. **88**, 163901 (2002).
7. E. H. K. Stelzer, "Beyond the diffraction limit?" Nature (London) **417**, 806–807 (2002).
8. M. G. Raymer, M. Beck, and D. F. McAlister, "Complex wave-field reconstruction using phase-space tomography," Phys. Rev. Lett. **72**, 1137–1140 (1994).
9. W. H. Richardson, "Bayesian-based iterative method of image restoration," J. Opt. Soc. Am. **62**, 55–59 (1972).
10. A. Messiah, *Quantum Mechanics* (North-Holland, Amsterdam, 1970).
11. P. A. M. Dirac, *The Principles of Quantum Mechanics*, 3rd ed. (Clarendon, Oxford, UK, 1958).
12. E. Wigner, "On the quantum correction for thermodynamic equilibrium," Phys. Rev. **40**, 749–759 (1932).
13. J. Ville, "Theorie et applications de la notion de signal analytique," Cables Transm. **2A**, 61–74 (1948).
14. A. S. Holevo, "Statistical decision theory for quantum systems," J. Multivar. Anal. **3**, 337–394 (1973).
15. C. W. Helstrom, *Quantum Detection and Estimation Theory* (Academic, New York, 1976).
16. D. L. Phillips, "A technique for the numerical solution of certain integral equations of the first kind," J. Assoc. Comput. Mach. **9**, 84–97 (1962).
17. S. Twomey, "On the numerical solution of Fredholm integral equations of the first kind by the inversion of the linear system produced by quadrature," J. Assoc. Comput. Mach. **10**, 97–101 (1963).
18. K. Miller, "Least squares methods for ill-posed problems with a prescribed bound," SIAM J. Math. Anal. **1**, 52–74 (1970).
19. A. N. Tikhonov and V. Y. Arsenin, *Solution of Ill-Posed Problems* (Wiley, New York, 1977).
20. G. E. Backus and F. Gilbert, "The resolving power of growth earth data," Geophys. J. R. Astron. Soc. **16**, 169–205 (1968).
21. G. E. Backus and F. Gilbert, "Uniqueness in the inversion of inaccurate gross earth data," Philos. Trans. R. Soc. London Ser. A **266**, 123–192 (1970).
22. R. W. Gerchberg, "Superresolution through error energy reduction," Opt. Acta **21**, 709–720 (1974).
23. B. R. Frieden, "Band-unlimited reconstruction of optical objects and spectra," J. Opt. Soc. Am. **57**, 1013–1019 (1967).
24. B. R. Frieden, "On arbitrarily perfect imagery with a finite aperture," Opt. Acta **16**, 795–807 (1969).
25. G. Toraldo di Francia, "Degrees of freedom of an image," J. Opt. Soc. Am. **59**, 799–804 (1969).
26. B. R. Frieden, "Evaluation, design and extrapolation methods for optical signals, based on use of the prolate functions," in *Progress in Optics, Vol. IX*, E. Wolf, ed. (North-Holland, Amsterdam, 1971), Chap. 8, pp. 311–407.
27. J. Peřina and V. Peřinová, "Optical imaging with partially coherent non-thermal light. II. Reconstruction of object from its image and similarity between object and its image," Opt. Acta **16**, 309–320 (1969).
28. J. Peřina, V. Peřinová, and Z. Braunerová, "Superresolution in linear systems with noise," Opt. Appl. **VII**, 79–83 (1977).
29. R. E. Burge, M. A. Fiddy, A. H. Greenaway, and G. Ross, "The application of dispersion relations (Hilbert transforms) to phase retrieval," J. Phys. D Appl. Phys. **7**, L65–L68 (1974).
30. R. E. Burge, M. A. Fiddy, A. H. Greenaway, and G. Ross, "The phase problem," Proc. R. Soc. London Ser. A **350**, 191–212 (1976).
31. R. W. Gerchberg and W. O. Saxton, "A practical algorithm for the determination of phase from image and diffraction plane pictures," Optik **35**, 237–246 (1972).
32. J. R. Fienup, "Phase retrieval algorithms: a comparison," Appl. Opt. **21**, 2758–2769 (1982).
33. D. C. Youla and H. Webb, "Image restoration by the method of convex projections: part I—theory," IEEE Trans. Med. Imaging **MI-1**, 81–94 (1982).
34. W. Kim, "Two-dimensional phase retrieval using a window function," Opt. Lett. **26**, 134–136 (2001).
35. R. W. Gerchberg, "A new approach to phase retrieval of a wave front," J. Mod. Opt. **49**, 1185–1196 (2002).
36. H. H. Bauschke, P. L. Combettes, and D. R. Luke, "Phase retrieval, error reduction algorithm, and Fienup variants: a view from convex optimization," J. Opt. Soc. Am. A **19**, 1334–1345 (2002).
37. M. R. Teague, "Irradiance moments: their propagation and use for unique retrieval of phases," J. Opt. Soc. Am. **72**, 1199–1209 (1982).
38. M. R. Teague, "Deterministic phase retrieval: a Green's function solution," J. Opt. Soc. Am. **73**, 1434–1441 (1983).
39. K. A. Nugent, T. E. Gureyev, D. F. Cookson, D. Paganin, and Z. Barnea, "Quantitative phase imaging using hard x rays, Phys. Rev. Lett. **77**, 2961–2964 (1996).

40. D. Paganin and K. A. Nugent, "Noninterferometric phase imaging with partially coherent light," Phys. Rev. Lett. **80**, 2586–2589 (1998).
41. L. J. Allen and M. P. Oxley, "Phase retrieval from series of images obtained by defocus variation," Opt. Commun. **199**, 65–75 (2001).
42. M. J. Bastiaans and K. B. Wolf, "Phase reconstruction from intensity measurements in linear systems," J. Opt. Soc. Am. A **20**, 1046–1049 (2003).
43. D. F. V. James and G. S. Agarwal, "Generalized Radon transform for tomographic measurement of short pulses," J. Opt. Soc. Am. B **12**, 704–708 (1995).
44. X. Liu and K.-H. Brenner, "Reconstruction of two-dimensional complex amplitudes from intensity measurements," Opt. Commun. **225**, 19–30 (2003).
45. J. Bertrand and P. Bertrand, "A tomographic approach to Wigner's function," Found. Phys. **17**, 397–405 (1987).
46. K. Vogel and H. Risken, "Determination of quasiprobability distribution in terms of probability distribution for the rotated quadrature phase," Phys. Rev. A **40**, 2847–2849 (1989).
47. D. T. Smithey, M. Beck, M. G. Raymer, and A. Faridani, "Measurement of the Wigner distribution and the density matrix of a light mode using optical homodyne tomography: application to squeezed states and the vacuum," Phys. Rev. Lett. **70**, 1244–1247 (1993).
48. C. Kurtsiefer, T. Pfau, and J. Mlynek, "Measurement of the Wigner function of an ensemble of helium atoms," Nature (London) **386**, 150–153 (1997).
49. G. T. Herman, *Image Reconstruction from Projections: The Fundamentals of Computerized Tomography* (Academic, New York, 1980).
50. A. C. Kak and M. Slaney, *Principles of Computerized Tomographic Imaging* (Institute of Electrical and Electronics Engineers, New York, 1988).
51. F. Natterer, *The Mathematics of Computerized Tomography* (Wiley, New York, 1986).
52. S. Quabis, R. Dorn, M. Eberler, O. Göckl, and G. Leuchs, "The focus of light—theoretical calculation and experimental tomographic reconstruction," Appl. Phys. B **72**, 109–113 (2001).
53. G. M. D'Ariano, C. Macchiavello, and M. G. A. Paris, "Detection of the density matrix through optical homodyne tomography without filtered back projection," Phys. Rev. A **50**, 4298–4302 (1994).
54. G. M. D'Ariano, C. Macchiavello, and M. G. A. Paris, "A fictitious photons method for tomographic imaging," Opt. Commun. **129**, 6–12 (1996).
55. S. Schiller, G. Breitenbach, S. F. Pereira, T. Muller, and J. Mlynek, "Quantum statistics of the squeezed vacuum by measurement of the density matrix in the number state representation," Phys. Rev. Lett. **77**, 2933–2936 (1996).
56. G. Breitenbach, S. Schiller, and J. Mlynek, "Measurement of the quantum states of squeezed light," Nature (London) **387**, 471–475 (1997).
57. A. I. Lvovsky, H. Hansen, T. Aichele, O. Benson, J. Mlynek, and S. Schiller, "Quantum state reconstruction of the single-photon Fock state," Phys. Rev. Lett. **87**, 050402-1-4 (2001).
58. S. Mancini, V. I. Man'ko, and P. Tombesi, "Wigner function and probability distribution for shifted and squeezed quadratures," Quantum Semiclassic. Opt. **7**, 615–623 (1995).
59. M. A. Man'ko, "Electromagnetic signal processing and noncommutative tomography," J. Russ. Laser Res. **23**, 433–448 (2002).
60. C. W. Helstrom, "Image restoration by the method of least squares," J. Opt. Soc. Am. **57**, 297–303 (1967).
61. Y. Biraud, "A new approach for increasing the resolving power by data processing," Astron. Astrophys. **1**, 124–127 (1969).
62. T. Opatrný, D. G. Welsch, and W. Vogel, "Least-squares inversion for density-matrix reconstruction," Phys. Rev. A **56**, 1788–1799 (1997).
63. A. P. Dempster, N. M. Laird, and D. B. Rubin, "Maximum likelihood from incomplete data via the EM algorithm," J. R. Stat. Soc. Ser. B **39**, 1–38 (1977).
64. R. A. Fisher, "On the mathematical foundations of theoretical statistics," Philos. Trans. R. Soc. London Ser. A **222**, 309–368 (1922).
65. R. A. Fisher, "Theory of statistical estimation," Proc. Cambridge Philos. Soc. **22**, 700–725 (1925).
66. A. Rockmore and A. Macovski, "A maximum likelihood approach to emission image reconstruction from projections," IEEE Trans. Nucl. Sci. **23**, 1428–1432 (1976).
67. L. A. Shepp and Y. Vardi, "Maximum likelihood reconstruction for emission tomography," IEEE Trans. Med. Imaging **1**, 113–122 (1982).
68. D. L. Snyder, M. I. Miller, J. L. J. Thomas, and D. G. Politte, "Noise and edge artifacts in maximum-likelihood reconstructions for emission tomography," IEEE Trans. Med. Imaging **6**, 228–238 (1987).
69. A. Rockmore and A. Macovski, "A maximum likelihood approach to transmission image reconstruction from projections," IEEE Trans. Nucl. Sci. **24**, 1929–1935 (1977).
70. J. Řeháček, Z. Hradil, M. Zawisky, W. Treimer, and M. Strobl, "Maximum likelihood absorption tomography," Europhys. Lett. **59**, 694–700 (2002).
71. Y. Vardi and D. Lee, "From image deblurring to optimal investments: Maximum likelihood solutions for positive linear inverse problems," J. R. Statist. Soc. B **55**, 569–612 (1993).
72. B. R. Frieden, "Applications to optics and wave mechanics of the criterion of maximum Cramer–Rao bound," J. Mod. Opt. **35**, 1297–1316 (1988).
73. B. R. Frieden, *Physics From Fisher Information. A Unification* (Cambridge U. Press, Cambridge, UK, 1998; reprinted 1999).
74. J. Řeháček and Z. Hradil, "Invariant information and quantum state estimation," Phys. Rev. Lett. **88**, 130401-1-4 (2002).
75. C. E. Shannon, "A mathematical theory of communication," Bell Syst. Tech. J. **27**, 379–423, 623–656 (1948).
76. E. T. Jaynes, "Information theory and statistical mechanics," Phys. Rev. **106**, 620–630; **108**, 171–190 (1957).
77. B. R. Frieden, "Restoring with maximum likelihood and maximum entropy," J. Opt. Soc. Am. **62**, 511–518 (1972).
78. S. F. Gull and G. J. Daniell, "Image reconstruction from incomplete and noisy data," Nature (London) **272**, 686–690 (1978).
79. B. R. Frieden and D. J. Graser, "Closed-form maximum entropy image restoration," Opt. Commun. **146**, 79–84 (1998).
80. V. Bužek, G. Adam, and G. Drobný, "Quantum state reconstruction and detection of quantum coherences on different observation levels," Phys. Rev. A **54**, 804–820 (1996).
81. Z. Hradil, "Quantum-state estimation," Phys. Rev. A **55**, R1561–R1564 (1997).
82. Z. Hradil, J. Summhammer, and H. Rauch, "Quantum tomography as normalization of incompatible observation," Phys. Lett. A **261**, 20–24 (1999).
83. Z. Hradil and J. Summhammer, "Quantum theory of incompatible observations," J. Phys. A Math. Gen. **33**, 7607–7612 (2000).
84. J. Řeháček, Z. Hradil, and M. Ježek, "Iterative algorithm for reconstruction of entangled states," Phys. Rev. A **63**, 040303-1-4 (2001).
85. M. Ježek, J. Fiurášek, and Z. Hradil, "Quantum inference of states and processes," Phys. Rev. A **68**, 012305-1-7 (2003).
86. K. Banaszek, G. M. D'Ariano, M. G. A. Paris, and M. F. Sacchi, "Maximum-likelihood estimation of the density matrix," Phys. Rev. A **61**, 010304-1-4 (2000).
87. Z. Hradil, J. Summhammer, G. Badurek, and H. Rauch, "Reconstruction of the spin state," Phys. Rev. A **62**, 014101 (2000).
88. S. A. Babichev, B. Brezger, and A. I. Lvovsky, "Remote preparation of a single-mode photonic qubit by measuring field quadrature noise," Phys. Rev. Lett. **92**, 047903-1-4 (2003).
89. A. I. Lvovsky, "Iterative maximum-likelihood reconstruction in quantum homodyne tomography" (2003); arXiv:quant-ph/0311097.

JOSA A

Optics, Image Science, and Vision

Volume 21
Number 8
August 2004

(Contents continued inside)

OSA® Optical Society of America